ADVANCED ELECTRONIC MATERIALS Open Access
www.advelectronicmat.de

Check for updates

Charge Transport in Blue Quantum Dot Light-Emitting Diodes

Shuxin Li, Wenxin Lin, Haonan Feng, Paul W. M. Blom, Jiangxia Huang, Jiahao Li, Xiongfeng Lin, Yulin Guo, Wenlin Liang, Longjia Wu, Quan Niu,* and Yuguang Ma*

Although quantum dot light-emitting diodes (QLEDs) are extensively studied nowadays, their charge transport mechanism remains a subject of ongoing debate. Here, the hole transport in blue quantum dots (QDs) (CdZnSe/ZnSe/ZnS/CdZnS/ZnS based) is investigated by combining current-voltage and transient electroluminescence measurements. The study demonstrates that the hole transport in QD thin films is characterized by a trap-free space-charge-limited current with a zero-field room temperature mobility of 4.4×10^{-11} m^2 V^{-1} s^{-1}. The zero-field hole mobility is thermally activated with an activation energy of 0.30 eV. Applying the Extended Gaussian Disorder model provides a consistent description of the QD hole current as a function of voltage and temperature. The QD hole mobility is characterized by a hopping distance of 2.8 nm in a Gaussian broadened density of states with a width of 0.12 eV.

1. Introduction

Quantum dot light-emitting diodes (QLEDs) are considered as the next-generation display technology due to the wide color gamut, pure color emission, large-area solution processability, and excellent size-dependent properties. However, the relatively low stability of such devices, especially blue QLEDs, suppresses their commercialization. For the improvement of device stability, it's critical to understand the degradation mechanism behind. Without an accurate description of charge transport, the degradation process of QLEDs cannot be quantified.

Previously, extensive studies on the charge transport of quantum dots (QDs) were carried out and different transport mechanisms were proposed.[1] On one hand, it was suggested that the charge transport is band-like. An increase in both the linear and saturation mobility in field-effect transistors (FET) was observed with decreasing temperature, which is the hallmark of band transport.[2] A similar result has also been obtained from the temperature dependence of the photoconductance.[3] It should be noted that in both measurements, the reported mobility of QDs is >10 cm^2 V^{-1} s^{-1}, indicative of strongly coupled and doped QDs. In such high-mobility QDs, a transition in the temperature dependence of the charge transport is observed; at high temperatures, the mobility increases with decreasing temperature, while at low temperatures, the mobility decreases with decreasing temperature. This has been attributed to a reduction in carrier concentration due to the presence of shallow traps. At high temperatures, all carriers can escape from the traps such that all carriers can be considered as free, and band-like transport is observed. At low temperatures the carrier concentration is reduced when lowering the temperature due to enhanced trapping, leading to a decrease in the transport thus leading to a transition in the transport mechanism.[2b] It should be noted that such a decrease is often expressed in terms of an effective mobility, although it stems from a decrease of the carrier concentration. Furthermore, Lan et al. use the fact that the ratio of electric Hall mobility (μ_{eHall}) and FET mobility (μ_{eFET}) is close to unity to explain the delocalization required for band-like transport.[4] However, a ratio close to unity can also be observed for ions in electrolytes, and this result alone can therefore not prove delocalization in QDs. As an alternative to the above-mentioned classical band-like transport including traps, phonon-assisted small polaron hopping models have been proposed based on theoretical simulations, but extensive experimental verification is still lacking.[5]

Alternatively, in the case of QDs without strong coupling and mobility significantly <10 cm^2 V^{-1} s^{-1}, hopping transport is considered to be appropriate. The observed temperature dependence of the conductivity in such QD films was attributed to the fact that the energy landscape of a QD array is inherently disordered.[6]

S. Li, W. Lin, H. Feng, J. Huang, J. Li, Q. Niu, Y. Ma
State Key Laboratory of Luminescent Materials and Devices
South China University of Technology
Guangzhou, Guangdong 510641, China
E-mail: qqniu@scut.edu.cn
P. W. M. Blom
Max Planck Institute for Polymer Research
Ackermannweg 10, 55128 Mainz, Germany
E-mail: blom@mpip-mainz.mpg.de
X. Lin, Y. Guo, W. Liang, L. Wu
TCL Corporate Research
Shenzhen, Guangdong 518067, China

The ORCID identification number(s) for the author(s) of this article can be found under https://doi.org/10.1002/aelm.202400142

© 2024 The Author(s). Advanced Electronic Materials published by Wiley-VCH GmbH. This is an open access article under the terms of the Creative Commons Attribution License, which permits use, distribution and reproduction in any medium, provided the original work is properly cited.

DOI: 10.1002/aelm.202400142

 © 2024 The Author(s). Advanced Electronic Materials published by Wiley-VCH GmbH

2199160x, 2024, 11, Downloaded from https://onlinelibrary.wiley.com/doi/10.1002/aelm.202400142 by MPI 355 Polymer Research, Wiley Online Library on [20/11/2024]. See the Terms and Conditions (https://onlinelibrary.wiley.com/terms-and-conditions) on Wiley Online Library for rules of use; OA articles are governed by the applicable Creative Commons License

Minute variations in the size, shape, and position of the nanocrystals result in differences in the energies of electrons (or holes) occupying the quantum-confined orbitals. In such disordered systems, charge transport is expected to take place via the variable-range hopping mechanisms.[6–7] Apart from the temperature dependence, Yu et al. found that the charge transport in quantum dots also depends on the applied electric field.[8] By studying the dependence of conductivity on temperature and electric field in n-type doped QD thin films, the charge transport characteristics of QD thin films were described. However, from conductivity measurements, it is hard to disentangle the effects of carrier concentration and charge carrier mobility. Instead of measuring the conductivity of QD thin films, Mentzel et al. investigated charge transport in a field-effect transistor.[9] By characterizing the current as a function of electric field and temperature, it was shown that QD solids are well described by a hopping model. However, the field dependence of hole mobility was not discussed. Furthermore, the annealing temperature appears to have some influence on the QD transport mechanism in FET devices.[10] QDs may melt or sinter at elevated temperatures, potentially causing alterations in the charge transport mechanisms within the QD structure. Further research is needed to draw conclusive results.

In addition to the aforementioned investigations conducted using FET devices or conventional thin films, there have been research efforts focusing on QD charge transport in the context of QLEDs. Ginger et al. studied the current-voltage characteristic of CdSe-based QLEDs with different electrode materials, QD sizes, and temperatures.[11] By fitting the current-voltage characteristic of QLEDs with a space-charge-limited current (SCLC) model considering deep traps, the electron mobility and trap density of the QD thin films were obtained. Furthermore, Hikmet et al. also obtained electron mobility and trap density of a QD layer by fitting the current-voltage characteristics of the QLED with a SCLC model.[12] However, in a QLED, the transport is bipolar, meaning it is dependent on both hole and electron transport. Furthermore, in such bipolar devices, the recombination process also strongly affects the device current. Therefore, it is hard to disentangle and understand the individual contributions of the electron or the hole transport and recombination by fitting the current density-voltage (J-V) characteristic of a bipolar device.

To understand the hole transport in QD thin films we fabricate hole-only devices based on $Cd_xZn_{1-x}Se/ZnSe/ZnS/CdZnS/ZnS$ QDs similar as used in conventional QLED devices. We investigate the charge transport in thin films and its dependence on electric field and temperature. We find that at low voltages the current depends quadratically on voltage, which is a fingerprint of a space-charge-limited current. By transient electroluminescent measurements, we confirm that the obtained SCLC room temperature mobility of 4.4×10^{-11} m^2 V^{-1} s^{-1} is not affected by trapping. Furthermore, the mobility is thermally activated with an activation energy of 0.30 eV, characteristic for hopping transport in a disorder broadened density of states. The extended Gaussian Disorder model (EGDM) is applied to model the J–V characteristics over the full voltage regime and provides information on the electric field, temperature, and charge carrier density dependence of the hole transport in QD thin films. This quantification will strongly support the understanding of the performance of QLEDs and their degradation process.

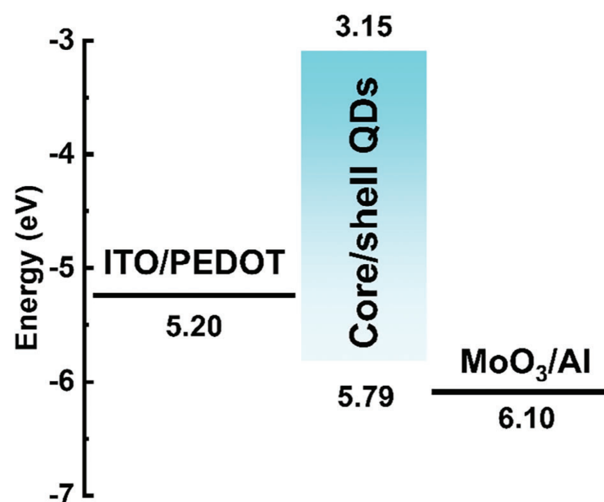

Figure 1. Device structure of hole-only devices: ITO/PEDOT:PSS/QDs/MoO_3/Al.

2. Results and Discussion

In this work, we fabricated hole-only devices based on QDs with a device structure consisting of indium tin oxide (ITO)/PEDOT:PSS/QDs/MoO_3/Al. The QDs used to fabricate the devices have a core/shell/shell structure of $Cd_xZn_{1-x}Se/ZnSe/ZnS/CdZnS/ZnS$ with a diameter of ≈6 nm. The outer thick shell of ZnS with a wide band gap, along with the use of capping ligands oleic acid (OA) and 1-dodecanethiol (DDT) as surface passivated materials, can enhance the stability of quantum dots (QDs). The thickness of the QD layer in the device was controlled at ≈110 nm to obtain an appropriate current density. To derive the charge transport properties of the QDs directly, we did not use any additional charge transport layer in the devices. For the hole-only devices, a huge electron injection barrier was formed by evaporating a layer of MoO_3 with a high work function on the QD layer. Furthermore, the work functions of the electrodes on both sides of the device are close to the valence band of the QDs, thereby preventing electron injection so that we can selectively study the bulk transport properties of holes in the device. The J–V measurements are performed in a nitrogen atmosphere in a temperature range of 217–297 K.

The device structure and energy diagram are shown in **Figure 1**. The energy level of QDs is determined by cyclic voltammetry in degassed dichloromethane solution at room temperature and the low-energy cutoff wavelength of the absorption spectrum (Figure S1, Supporting Information). To achieve efficient hole injection the high work function electrode MoO_3 (6.1 eV) is applied. The hole-only devices thus comprised a single layer of QD material sandwiched between a PEDOT:PSS bottom electrode and a MoO_3/Al top electrode (Figure 1).

In **Figure 2a** the log-log J–V characteristic is shown for positive bias, corresponding to hole injection from the MoO_3 contact. From the slope of the $\log J - \log V$ plot (Figure 2a), we observe that the current density J depended quadratically on the voltage V at low bias voltage. This behavior is the characteristic of a

 © 2024 The Author(s). Advanced Electronic Materials published by Wiley-VCH GmbH

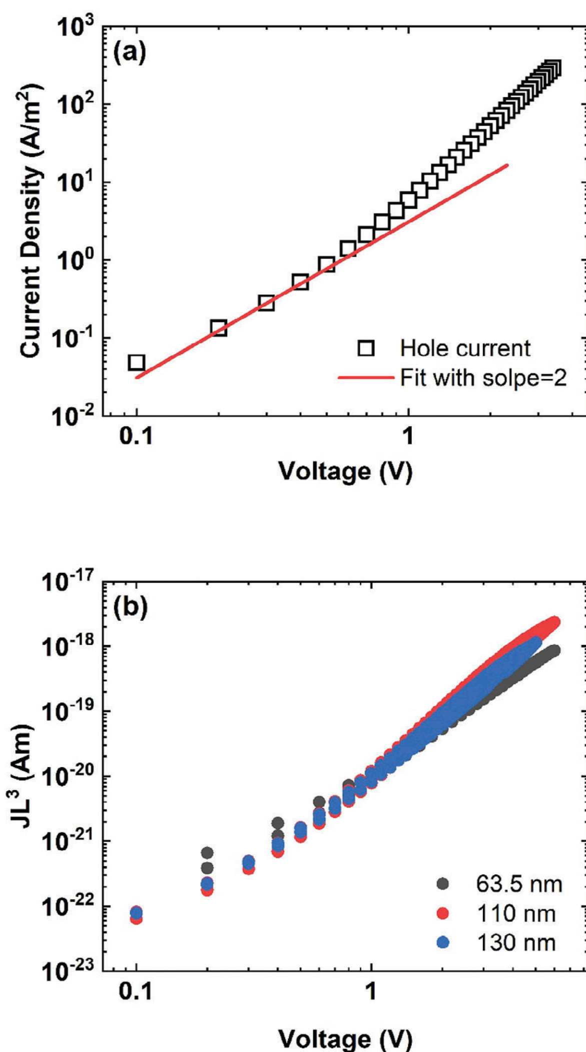

Figure 2. a) Current density J versus voltage V of a hole-only device with thicknesses L = 110 nm, measured at room temperature. The solid line represents the calculated SCLC (Equation (1)) with μ (0)= 4.4 × 10^{-11} m^2 V^{-1} s^{-1}. b) JL^3–V curves of hole-only devices of different thicknesses.

space-charge-limited current, with the current density described by the Mott–Gurney law,[13]

$$J = \frac{9}{8}\, \varepsilon_0 \varepsilon_r \mu \frac{V^2}{L^3} \tag{1}$$

with ϵ_0 the vacuum permittivity, ϵ_r the relative permittivity, μ the mobility (here the hole mobility), V the voltage and L the thickness of the QD layer. The observation of space-charge-limited current enables us to obtain the charge carrier mobility directly from the J–V characteristics. The calculated (low field) charge-carrier mobility $\mu(0)$ is 4.4×10^{-11} m^2 V^{-1} s^{-1}. In order to further confirm whether the injected hole currents are truly space-charge limited, it is imperative to examine the thickness dependence of the hole current. Figure 2b shows the JL^3–V curves of three hole-only devices of different thicknesses. Since the measurements converge onto a singular curve, this observation suggests that the current inversely correlates with the cube of the layer thickness. Combined with the quadratic dependence on voltage this unequivocally confirms that the injected current is space-charge limited.

However, a fundamental question remains, namely whether the obtained mobility is a drift mobility or an effective mobility. In the case of shallow hole traps the current-voltage characteristics are given by[14]

$$J = \frac{9}{8}\, \varepsilon_0 \varepsilon_r \theta \mu \frac{V^2}{L^3} \tag{2}$$

where θ represents the proportion between the free hole carrier density p and the total injected hole density p+p_t, where p_t is the density of trapped holes that do not contribute to the current. The product $\theta\mu$ is typically termed “effective mobility”. Also, this trap-limited J–V characteristic exhibits a quadratic voltage dependence and inverse cube law on sample thickness, similar to the classical SCLC (Equation (1)). The fundamental difference is that in case of the classical SCLC (Equation (1)) all carriers move with a velocity of $v = \mu E$, with E the applied electric field, whereas for the trap-limited current only a small fraction θ of the injected carriers can move with a mobility μ, whereas the majority of injected carriers resides in traps. Applying Equation (1) to this case would underestimate the mobility of the free carriers by orders of magnitude. Which mechanism applies to the QDs is also relevant to understand the enhancement of the current at higher voltages, where it rises more steeply than quadratic with voltage. In the classical case, the mobility is enhanced by the electric field and carrier density, whereas in the trap-limited case more carriers can escape from the traps at higher electric field due to the Poole–Frenkel effect. In that case, the enhancement of the current is a carrier density effect and not a mobility effect.

To disentangle whether the obtained mobility is the average mobility resulting from hopping transport or an effective mobility governed by shallow traps we have performed transient experiments in order to determine the hole transit time τ_d. In case that the classical SCLC model applies, the mobility obtained from the hole transit time

$$\mu = \frac{L^2}{\tau_d V} \tag{3}$$

equals the mobility obtained from SCLC. In contrast, for the trap-limited case the transient mobility will be much higher than the effective ($\theta\mu$) SCLC mobility, since the transit time is governed by the mobility μ of the small fraction of free carriers. Typically, time-of-flight measurements (TOF) are used to determine the charge carrier mobility via Equation (3) in disordered systems. However, due to the often highly dispersive transient photocurrent traces in low mobility materials, the determination of charge-carrier mobilities can be complicated and at low fields practically impossible.[15] Therefore, we use transient electroluminescence (TEL) measurements to measure and investigate the electric field dependence of the hole mobility. In contrast to TOF measurements, which need a relatively thick semiconductor film (approximately μm in thickness), TEL can be directly used in conventional QLEDs featuring a film thickness of ≈100 nm. In TEL measurements, there is a time lag between the application of a voltage pulse and the onset of the electroluminescence (EL) of devices. The observed time lag (τ_d) is equal to the transit time

© 2024 The Author(s). Advanced Electronic Materials published by Wiley-VCH GmbH

2199160x, 2024, 11, Downloaded from https://onlinelibrary.wiley.com/doi/10.1002/aelm.202400142 by MPI 355 Polymer Research, Wiley Online Library on [20/11/2024]. See the Terms and Conditions (https://onlinelibrary.wiley.com/terms-and-conditions) on Wiley Online Library for rules of use; OA articles are governed by the applicable Creative Commons License

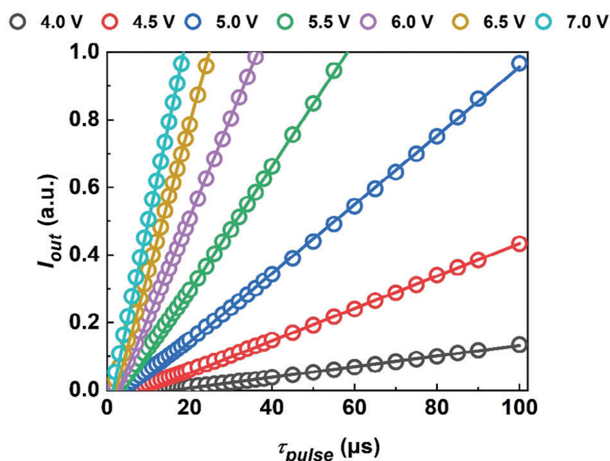

Figure 3. Time-integrated light output I_{out} versus voltage pulse length τ_{pulse} for a QLED at $T = 297$ K.

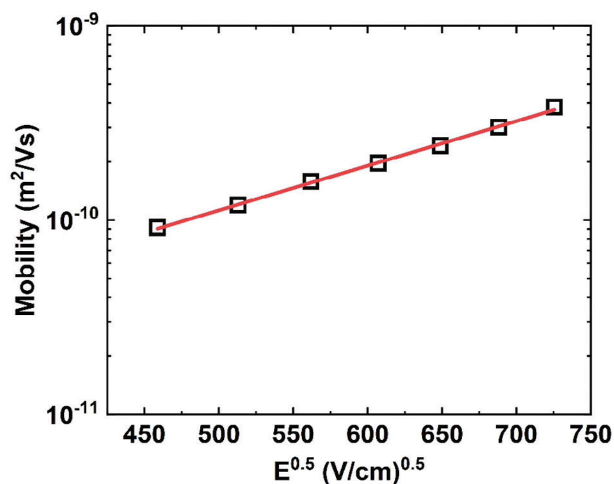

Figure 4. Hole mobility calculated from the observed response times in transient electroluminescence measurements as a function of the square of electric field. The solid line is a guide to the eye.

of charge carriers (Figure S3, Supporting Information). Within the context of a TEL measurement, as shown in **Figure 3**, a rectangular voltage pulse is administered to the QLED, varying in duration. In case that charge transport is unbalanced, the measured transit time τ_d is correlated with the transit time of the fastest charge carrier. In an earlier study, we fabricated hole-only devices and electron-only devices without charge transport layer, with the structures of ITO/PEDOT:PSS/QDs (100 nm)/MoO_3/Al and Al/QDs (100 nm)/LiF/Al, respectively.[16] By comparing the different between hole and electron current, we have found that the holes are the dominant and fastest carrier in our QD system. By comparing the different between hole and electron current, we have found that the holes are the dominant and fastest carrier in our QD system. Therefore, in a QLED, following the application of voltage, the holes embark on a journey from the anode to the cathode. After a finite transit time τ_d the holes reach the recombination zone at the cathode where they meet with the slow electrons and electroluminescence is generated. Consequently, the delay time τ_d between the commencement of the voltage pulse and the initiation of light emission served as an indicator of the hole transit time.[17] Using the TEL method, shown in Figure 3, we analyzed the transit time of holes in QLEDs as a function of applied voltage. The resulting transient hole mobility is plotted in **Figure 4**. At an applied voltage of 4 V ($E^{0.5} = 458.8$ (V cm^{-1})$^{0.5}$) the obtained hole mobility amounts to 9.1×10^{-11} m^2 V^{-1} s^{-1}. From the J–V characteristics, we observe that at the same electric field the current is outside the quadratic regime and is about five times larger than the predicted quadratic SCLC (Equation (1)) using a mobility of 4.4×10^{-11} m^2 V^{-1} s^{-1}. The estimated SCLC mobility at the same electric field is therefore close to 2.2×10^{-10} m^2 V^{-1} s^{-1} and is in excellent agreement with the TEL mobility. This agreement between SCLC and transient mobility demonstrates that the observed J–V characteristics represent the classical trap-free SCLC.

Having established that the room temperature mobility is not an effective trap-limited mobility but the intrinsic drift mobility we now investigate the temperature dependence of the charge transport. As a first step, we determine the low field mobility $\mu(0)$ from the quadratic part of the J–V characteristics as a function of temperature. The resulting Arrhenius plot is shown in **Figure 5**. The thermally activated charge transport is described as:

$$\mu(0) = \mu_\infty \exp\left(-\frac{\Delta}{k_B T}\right) \tag{4}$$

Equation (4) provides a good description of the temperature dependence of the mobility with prefactor $\mu_\infty = 4.5 \times 10^{-6}$ m^2 V^{-1} s^{-1} and activation energy $\Delta = 0.30$ eV (Figure 5). A similar temperature dependence was also observed in previous studies on charge transport in QDs.[7b] The strong temperature dependence further indicates that the charge transport in our QD thin film is mainly governed by hopping. The activation energy in QDs is smaller than polymer (PPV ≈0.48 eV), which means the energetic disorder in QDs is smaller than polymer, leading to larger mobility.[15]

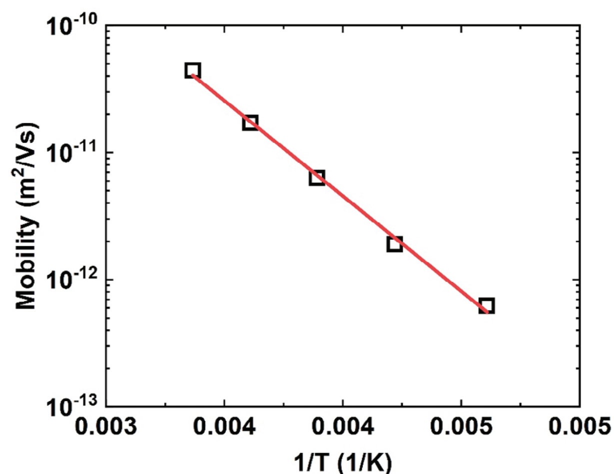

Figure 5. Arrhenius plot of the zero-field mobility versus temperature. The zero-field mobility is obtained from the experimental J-V characteristics using Equation (1). The solid line is fitting by Equation (4) and corresponds with an activation energy of 0.30 eV.

© 2024 The Author(s). Advanced Electronic Materials published by Wiley-VCH GmbH

2199160x, 2024, 11, Downloaded from https://onlinelibrary.wiley.com/doi/10.1002/aelm.202400142 by MPI 355 Polymer Research, Wiley Online Library on [20/11/2024]. See the Terms and Conditions (https://onlinelibrary.wiley.com/terms-and-conditions) on Wiley Online Library for rules of use; OA articles are governed by the applicable Creative Commons License

Besides temperature and electric field, the carrier density can also influence the hopping transport in an energetically disordered system, as in the case of organic semiconductors with disordered energy distribution.[18] Here, due to the weak intermolecular interaction, the charge carriers need to "hop" from one localized energy site to another with the assistance of a phonon.[19] The electrical field and temperature dependence of hopping transport in organic semiconductors has been extensively studied. By taking into account the density-, field- and temperature dependence of mobility and solving the master equation for hopping transport in Gaussian distributed energy sites, Pasveer et al. proposed the Extended Gaussian Disorder Model to describe the charge carrier mobility in organic semiconductors, which provided a consistent description of the trap-free charge transport in large range organic semiconductors.[18a]

In our case, quantum dots are nanocrystals with a size of 2–20 nm. The composition, size, shape, and spacing of the quantum dots will all influence the transport properties.[20] It is hard to achieve quantum dots dispersed in a solvent with homogeneous composition, size, shape, and spacing.[21] Furthermore, to improve the solubility and stability of quantum dots, organic molecules are always introduced as ligands to quantum dots, which further weaken the interaction between the QDs.[1b,22] At the same time, the undercoordinated surface atoms with dangling bonds always act as traps in QDs.[22] These factors cause localization and disorder of the energy sites in the QD system, resulting in hopping dominated transport of charge carriers.

Following the formalism developed for disordered organic semiconductors we apply the Extended Gaussian Distribution model, which simultaneously contains the electric field, temperature, and charge carrier density dependence of the charge carrier mobility, to the charge transport in our quantum dot thin films.[18a] In the EGDM the mobility is given by

$$\mu\,(T, p, E) \;=\mu_p\;\,(T, p)\,\mu_E\,(T, E) \tag{5a}$$

where

$$\mu_p\;\,(T, p) = \mu_0\;\exp\left(-0.42\left(\frac{\sigma}{k_B T}\right)^2 + \frac{1}{2}\left(\left(\frac{\sigma}{k_B T}\right)^2 - \frac{\sigma}{k_B T}\right)\left(2pa^3\right)^{\delta}\right) \tag{5b}$$

and

$$\mu_E\,(T, E) \;= \exp\left(0.44\left(\left(\frac{\sigma}{k_B T}\right)^{3/2} - 2.2\right)\sqrt{1 + 0.8\left(\frac{Eea}{\sigma}\right)^2 - 1}\right) \tag{5c}$$

The exponent δ is given by:

$$\delta \;=\; 2\frac{\ln\left(\left(\sigma k_B T\right)^2 - \sigma/k_B T\right) - \ln\left(\ln 4\right)}{\left(\sigma/k_B T\right)^2} \tag{5d}$$

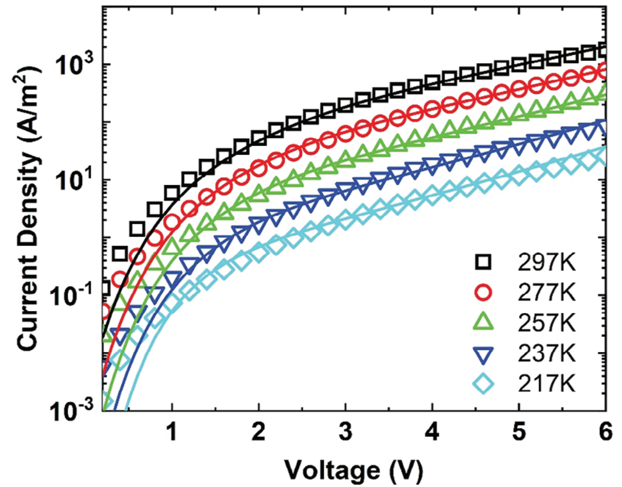

Figure 6. Current density J versus voltage V of a hole-only device with thickness L = 110 nm for various temperatures. The solid lines are the fits from the EGDM model.

p represents the hole density, σ is the width of the Gaussian density of states (DOS), and a the hopping distance. By numerically solving the current density and Poisson equation in combination with the EGDM mobility the J–V characteristics can be calculated. As **Figure 6** shows, the J–V characteristic of the hole transport in $Cd_xZn_{1-x}Se$-based quantum dot thin films can be well described at different temperatures by the EGDM, including the high voltage regime.

Furthermore, we can obtain the hopping distance a of charge carriers as the transport in quantum dot thin films, which amounts to 2.8 nm. This hopping distance is physically reasonable, which corresponds to the average distance between two quantum dots (Figure S2, Supporting Information). As discussed before, due to the differences in the size, shape, and trap sites of quantum dots, the energy distribution of quantum dots is disordered, with a width of the Gaussian distribution of energy sites of 0.12 eV, which is obtained from the EGDM fit.

Understanding of the transport mechanism in the blue quantum dot thin film will quantitatively support our understanding of the device operation of blue QLEDs. As a next step, radiative recombination rates, nonradiative recombination processes, and the aging mechanism of such devices have to be determined. This information is important to improve the stability of blue QLEDs, paving the way to their commercialization. The hopping transport as observed in the QDs under study is the result of the weak interaction between QDs, which leads to the localized energy distribution. Therefore, a possible way to increase the mobility of charge transport in quantum dot films is to increase the interaction between the QDs of the system.

3. Conclusion

In conclusion, we have investigated the charge transport in a blue QD thin film. By fabricating hole-only devices based on $Cd_xZn_{1-x}Se/ZnSe/ZnS/CdZnS/ZnS$ blue QDs. The current-voltage characteristics are characterized by a trap-free space-charge-limited current, evidenced by the agreement between the

 © 2024 The Author(s). Advanced Electronic Materials published by Wiley-VCH GmbH

2199160x, 2024, 11, Downloaded from https://onlinelibrary.wiley.com/doi/10.1002/aelm.202400142 by MPI 355 Polymer Research, Wiley Online Library on [20/11/2024]. See the Terms and Conditions (https://onlinelibrary.wiley.com/terms-and-conditions) on Wiley Online Library for rules of use; OA articles are governed by the applicable Creative Commons License

ADVANCED ELECTRONIC MATERIALS Open Access
www.advelectronicmat.de

SCLC and transient mobility. Furthermore, from the temperature dependence, we find a thermally activated hopping transport of holes in blue QD thin films with an activation energy of $\Delta = 0.30$ eV. Furthermore, the electric field, temperature, and charge carrier density dependence of the hole transport in QD thin films is well described by the Extended Gaussian Disorder Model. The understanding of the transport mechanism in such a system paves the way to quantitatively analyze the performance and the degradation mechanism of QLEDs.

4. Experimental Section

Material and Hole-Only device Fabrication: The quantum dots used to fabricate the hole-only devices had a core/shell/shell structure of $Cd_xZn_{1-x}Se$/ZnSe/ZnS/CdZnS/ZnS with a diameter of ≈6 nm. The ligands of quantum dots were oleic acid (OA) and 1-dodecanethiol (DDT). The photoluminescence (PL) and electroluminescence (EL) spectra are illustrated in the Figure S4 (Supporting Information). To fabricate hole-only devices, quantum dots dissolved in octane were spin-coated on a glass/indium tin oxide (ITO)/PEDOT:PSS substrate. The thickness of the QD layer is in the range of 63.5–130 nm. The MoO_3 (10 nm) and Al cathode (100 nm) were then thermally evaporated on top of the quantum dot layer (chamber pressure 10^{-7} mbar). The corresponding device architectures used in this study are ITO/PEDOT:PSS/QDs/MoO_3/Al.

Device Characterization: The current density-voltage (J–V) measurements were conducted in nitrogen atmosphere with a Keithley 2400 source meter. These measurements were performed at a temperature range of 217–297 K. To measure the transit time (τ) of charge carriers in quantum dot light-emitting diodes, an ITO/PEDOT:PSS (25 nm)/TFB (25 nm)/QD (30 nm)/ZnMgO (40 nm)/Ag QLED was used as a test device. A pulse generator (GW INSTEK MFG-2230M) was utilized to input a voltage pulse, resulting in a light output pulse. The width of the voltage pulse τ_{pulse} was increased from 2 to 100 µs, and the pulse amplitudes were varied gradually from 4 to 7 V with a 0.5 V step. The pulse period was set to be 1 ms. The integrated light output (I_{out}) was measured by a Keithley 6514 electrometer in current mode. When $\tau_{pulse} >> \tau$, a linear relation between I_{out} and τ_{pulse} would be obtained, and the intercept of the linear part with the τ_{pulse}-axis corresponds to τ.

Supporting Information

Supporting Information is available from the Wiley Online Library or from the author.

Acknowledgements

S.L. and W.L. contributed equally to this work. This work was funded by TCL Corporate Research, the National Natural Science Foundation of China (52103207), the Natural Science Foundation of Guangdong Province (2022A1515011969), and the Fundamental Research Funds for the Central Universities (2023ZYGXZR025).

Conflict of Interest

The authors declare no conflict of interest.

Data Availability Statement

The data that support the findings of this study are available from the corresponding author upon reasonable request.

Keywords

blue quantum dots, extended Gaussian disorder model, hopping transport, trap-free space-charge-limited current

Received: February 24, 2024
Revised: May 22, 2024
Published online: June 28, 2024

[1] a) X. Dai, Y. Deng, X. Peng, Y. Jin, *Adv. Mater.* **2017**, *29*, 1607022; b) F. P. García de Arquer, D. V. Talapin, V. I. Klimov, Y. Arakawa, M. Bayer, E. H. Sargent, *Science* **2021**, *373*, eaaz8541.
[2] a) J. S. Lee, M. V. Kovalenko, J. Huang, D. S. Chung, D. V. Talapin, *Nat. Nanotechnol.* **2011**, *6*, 348; b) J.-H. Choi, A. T. Fafarman, S. J. Oh, D.-K. Ko, D. K. Kim, B. T. Diroll, S. Muramoto, J. G. Gillen, C. B. Murray, C. R. Kagan, *Nano Lett.* **2012**, *12*, 2631; c) M. Scheele, *Z. Phys. Chem.* **2015**, *229*, 167; d) C. R. Kagan, C. B. Murray, *Nat. Nanotechnol.* **2015**, *10*, 1013.
[3] E. Talgorn, Y. Gao, M. Aerts, L. T. Kunneman, J. M. Schins, T. J. Savenije, M. A. van Huis, H. van der Zant, A. J. Houtepen, L. D. A. Siebbeles, *Nat. Nanotechnol.* **2011**, *6*, 733.
[4] X. Lan, M. Chen, M. H. Hudson, V. Kamysbayev, Y. Wang, P. Guyot-Sionnest, D. V. Talapin, *Nat. Mater.* **2020**, *19*, 323.
[5] a) I.-H. Chu, M. Radulaski, N. Vukmirović, H.-P. Cheng, L.-w. Wang, *J. Phys. Chem. C* **2011**, *115*, 21409; b) N. Prodanovic, N. Vukmirovic, Z. Ikonic, P. Harrison, D. Indjin, *J. Phys. Chem. Lett.* **2014**, *5*, 1335; c) N. Yazdani, S. Andermatt, M. Yarema, V. Farto, M. H. Bani-Hashemian, S. Volk, W. M. Lin, O. Yarema, M. Luisier, V. Wood, *Nat. Commun.* **2020**, *11*, 2852.
[6] A. J. Houtepen, D. Kockmann, D. Vanmaekelbergh, *Nano Lett.* **2008**, *8*, 3516.
[7] a) B. Skinner, T. Chen, B. I. Shklovskii, *Phys. Rev. B* **2012**, *85*, 205316; b) P. Guyot-Sionnest, *J. Phys. Chem. Lett.* **2012**, *3*, 1169.
[8] D. Yu, C. Wang, B. L. Wehrenberg, P. Guyot-Sionnest, *Phys. Rev. Lett.* **2004**, *92*, 216802.
[9] T. Mentzel, V. Porter, S. Geyer, K. MacLean, M. G. Bawendi, M. Kastner, *Phys. Rev. B* **2008**, *77*, 075316.
[10] H. E. Romero, M. Drndic, *Phys. Rev. Lett.* **2005**, *95*, 156801.
[11] D. Ginger, N. Greenham, *J. Appl. Phys.* **2000**, *87*, 1361.
[12] R. Hikmet, D. Talapin, H. Weller, *J. Appl. Phys.* **2003**, *93*, 3509.
[13] N. F. Mott, R. W. Gurney, *Electronic Process in Ionic Crystal*, Oxford University Press, Oxford 1940.
[14] M. A. Lampert, P. Mark, *Electrical Sci.* **1970**, *21*, 558.
[15] P. W. Blom, M. de Jong, M. van Munster, *Phys. Rev. B* **1997**, *55*, R656.
[16] W. Lin, J. Huang, S. Li, P. W. M. Blom, H. Feng, J. Li, X. Lin, Y. Guo, W. Liang, L. Wu, Q. Niu, Y. Ma, *J. Appl. Phys.* **2024**, *135*, 045701.
[17] P. Blom, M. Vissenberg, *Phys. Rev. Lett.* **1998**, *80*, 3819.
[18] a) W. Pasveer, J. Cottaar, C. Tanase, R. Coehoorn, P. Bobbert, P. Blom, D. De Leeuw, M. Michels, *Phys. Rev. Lett.* **2005**, *94*, 206601; b) M. Kuik, G. J. A. Wetzelaer, H. T. Nicolai, N. I. Craciun, D. M. De Leeuw, P. W. Blom, *Adv. Mater.* **2014**, *26*, 512; c) C. Tanase, E. Meijer, P. Blom, D. De Leeuw, *Phys. Rev. Lett.* **2003**, *91*, 216601; d) M. Vissenberg, M. Matters, *Phys. Rev. B* **1998**, *57*, 12964; e) P. Blom, C. Tanase, D. De Leeuw, R. Coehoorn, *Appl. Phys. Lett.* **2005**, *86*, 92105; f) C. Tanase, P. Blom, D. De Leeuw, *Phys. Rev. B* **2004**, *70*, 193202.
[19] a) E. M. Conwell, *Phys. Rev.* **1956**, *103*, 51; b) N. Mott, *Can. J. Phys.* **1956**, *34*, 1356.
[20] C. R. Kagan, C. B. Murray, *Nat. Nanotechnol.* **2015**, *10*, 1013.
[21] C. Murray, D. J. Norris, M. G. Bawendi, *J. Am. Chem. Soc.* **1993**, *115*, 8706.
[22] M. A. Boles, D. Ling, T. Hyeon, D. V. Talapin, *Nat. Mater.* **2016**, *15*, 141.

© 2024 The Author(s). Advanced Electronic Materials published by Wiley-VCH GmbH

2199160x, 2024, 11, Downloaded from https://onlinelibrary.wiley.com/doi/10.1002/aelm.202400142 by MPI 355 Polymer Research, Wiley Online Library on [20/11/2024]. See the Terms and Conditions (https://onlinelibrary.wiley.com/terms-and-conditions) on Wiley Online Library for rules of use; OA articles are governed by the applicable Creative Commons License